Cell, Vol. 89, 239–250, April 18, 1997, Copyright ©1997 by Cell Press

Crystal Structure of an Hsp90–Geldanamycin Complex: Targeting of a Protein Chaperone by an Antitumor Agent

Charles E. Stebbins,*‖ Alicia A. Russo,†‖ Christine Schneider,‡ Neal Rosen,§ F. Ulrich Hartl,‡ and Nikola P. Pavletich†

*Department of Biochemistry and Structural Biology
Cornell University Graduate School of Medical Sciences
New York, New York 10021

†Cellular Biochemistry and Biophysics Program
Memorial Sloan-Kettering Cancer Center
New York, New York 10021

‡Cellular Biochemistry and Biophysics Program and Howard Hughes Medical Institute
Memorial Sloan-Kettering Cancer Center
New York, New York 10021

§Cell Biology and Genetics Program and Department of Medicine
Memorial Sloan-Kettering Cancer Center
New York, New York 10021

Summary

The Hsp90 chaperone is required for the activation of several families of eukaryotic protein kinases and nuclear hormone receptors, many of which are proto-oncogenic and play a prominent role in cancer. The geldanamycin antibiotic has antiproliferative and antitumor effects, as it binds to Hsp90, inhibits the Hsp90-mediated conformational maturation/refolding reaction, and results in the degradation of Hsp90 substrates. The structure of the geldanamycin-binding domain of Hsp90 (residues 9–232) reveals a pronounced pocket, 15 Å deep, that is highly conserved across species. Geldanamycin binds inside this pocket, adopting a compact structure similar to that of a polypeptide chain in a turn conformation. This, and the pocket's similarity to substrate-binding sites, suggest that the pocket binds a portion of the polypeptide substrate and participates in the conformational maturation/refolding reaction.

Introduction

Geldanamycin, and its closely related analogs herbimycin and macbecin, are naturally occurring antitumor antibiotics (DeBoer et al., 1970; Omura et al., 1979; Ono et al., 1982). In the National Cancer Institute's (NCI) in vitro screen for antitumor agents, geldanamycin has shown potent activity, achieving 50% growth inhibition (GI_{50}) at concentrations as low as 13 nM against the most responsive cell lines, with a mean GI_{50} of 180 nM against all 60 of the tumor cell lines (Supko et al., 1995). Geldanamycin is active in mouse tumor models as well (Sasaki et al., 1979; Ono et al., 1982), and it has been selected for preclinical development as an antitumor agent by the NCI (Supko et al., 1995).

‖These authors contributed equally to this work.

The antitumor effects of geldanamycin likely result from its ability to deplete cells of two broad classes of growth-regulatory signaling proteins: (1) proto-oncogenic protein kinases, including the erbB2 (Miller et al., 1994; Chavany et al., 1996) and EGF (Murakami et al., 1994) receptor tyrosine kinases, the v-src family of nonreceptor tyrosine kinases (June et al., 1990; Xu and Lindquist, 1993; Hartson and Matts, 1994; Whitesell et al., 1994), and the Raf-1 (Schulte et al., 1995; Schneider et al., 1996) and CDK4 Ser/Thr kinases (Stepanova et al., 1996), whose overexpression, or otherwise deregulation, has been observed in diverse human cancers (Bouchard et al., 1989; Hunter and Pines, 1994; Tronick and Aaronson, 1995); and (2) the nuclear hormone receptor family, including the estrogen and androgen hormone receptors (Smith et al., 1995; Nair et al., 1996; Whitesell and Cook, 1996), which can drive the growth of hormone-dependent cancers of the breast (Osborne et al., 1980) and prostate (Isaacs and Coffey, 1979), respectively.

Initially thought to be a nonspecific kinase inhibitor, geldanamycin's target has only recently been identified as the heat shock protein Hsp90 (Whitesell et al., 1994) and its endoplasmic reticulum homolog GP96 (Chavany et al., 1996). In eukaryotes, Hsp90 has dual chaperone functions participating both in the conformational maturation of the nuclear hormone receptors and the aforementioned protein kinases, and in the cellular stress response (Bohen and Yamamoto, 1994; Jakob and Buchner, 1994; Pratt and Welsh, 1994). These two processes are likely to have in common the ability of Hsp90, in cooperation with Hsp70 and other factors, to prevent protein aggregation and mediate the ATP-dependent refolding of heat-denatured proteins in vitro and in vivo (Freeman and Morimoto, 1996; Schneider et al., 1996).

The best-studied Hsp90-mediated conformational maturation is that of the nuclear hormone receptors, which require the Hsp90 system in order to acquire or maintain a state competent to bind hormone (Bresnick et al., 1989; Picard et al., 1990; Nathan and Lindquist, 1995). In this ATP-dependent reaction, an initial hormone receptor complex that contains Hsp90, Hsp70, and at least two cochaperones, p60 and Hip (p48), is in equilibrium with a complex in which the receptor is in a metastable, nearly mature state competent to bind hormone (Smith et al., 1995; Dittmar et al., 1996). This nearly mature complex lacks Hsp70, p60, and Hip, but contains two new proteins, p23 and one of the three large immunophilins, FKBP52, FKBP54, or CyP40 (Smith et al., 1995; Dittmar et al., 1996). Upon hormone binding, the receptor is released as an active transcription factor (Smith et al., 1995; Dittmar et al., 1996). Treatment with geldanamycin appears to block the conversion to the nearly mature complex, preventing hormone binding and activation, and results in the degradation of the hormone receptor (Whitesell and Cook, 1996).

The requirement for Hsp90 in the activation of the aforementioned protein kinases has been demonstrated both genetically (Xu and Lindquist, 1993; Aligue et al., 1994; Nathan and Lindquist, 1995) and biochemically

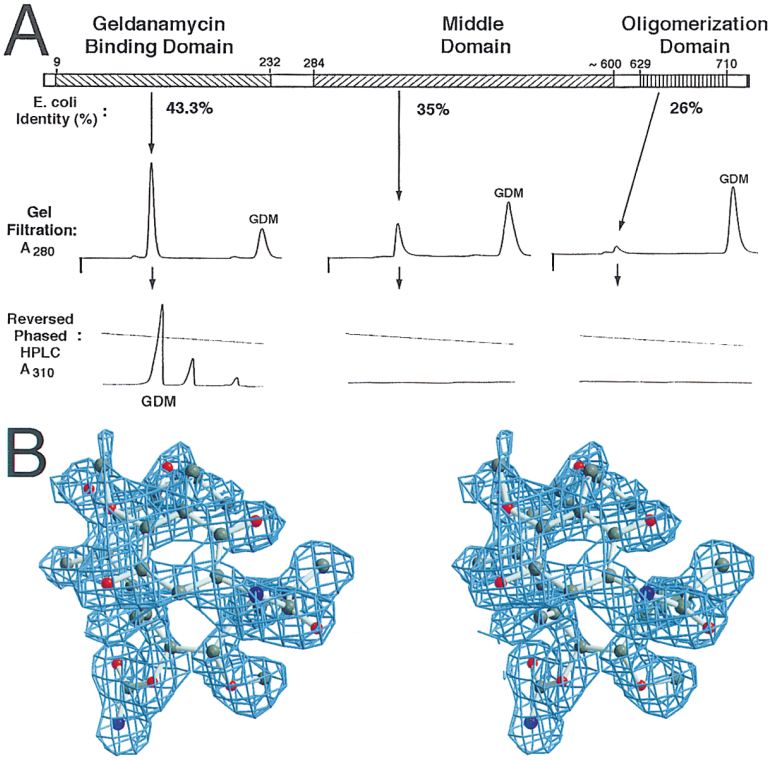

Figure 1. Geldanamycin Binds the N-Terminal Structural Domain of Hsp90

(A) The three structural domains of Hsp90, identified by proteolytic digestion, are indicated, together with their percent identity in the E. coli homolog. The oligomerization activity at the C-terminal portion has been described (Wearsch and Nicchitta, 1996). The digestion of residues 1–9 is consistent with this region being absent from most Hsp90 sequences except mammalian ones. To identify the geldanamycin-binding domain, the purified structural domains, at 1 μM, were incubated with 2.0 μM geldanamycin (GIBCO-BRL) each; the free drug was then separated on a gel filtration column, monitoring absorption at 280 nm, and the protein peaks (the C-terminal domain absorbed weakly at 280 nm for lack of tryptophans) were analyzed for the presence of geldanamycin by reverse-phase HPLC, with monitoring at 310 nm. The gel filtration protein peak of the N-terminal domain was the only one that contained geldanamycin; the molar ratio was determined to be approximately 1:1 based on UV absorption. The composition of the two secondary geldanamycin peaks observed in the reversed phase chromatography is not clear, but they could also be produced by the addition of dithiothreitol in the absence of protein. Geldanamycin is abbreviated as GDM.

(B) Stereo view of the geldanamycin 2Fo-Fc electron density before any geldanamycin atoms were built into the Hsp90 model. The map was calculated at 2.0 Å and contoured at 1.0 sigma; also shown is the refined geldanamycin model in a ball-and-stick representation.

(Hartson and Matts, 1994; Chavany et al., 1996; Stepanova et al., 1996). This reaction is not as well understood, but it appears to involve a subset of the molecules found in the complexes with hormone receptors, as well as a protein kinase–specific cofactor, $p50^{Cdc37}$ (Whitelaw et al., 1991; Stancato et al., 1993; Cutforth and Rubin, 1994; Stepanova et al., 1996). For some of these kinases, such as Raf-1, Hsp90 association is a prerequisite for their trafficking to the plasma membrane (Schulte et al., 1995); for others, the mechanism of Hsp90-mediated activation is not yet understood. Again, geldanamycin interferes with Hsp90 function and induces the rapid degradation of these kinases by the proteosome system (Murakami et al., 1994; Schulte et al., 1995; Schneider et al., 1996; Stepanova et al., 1996).

In addition to its role in the conformational maturation of signal transduction molecules, the eukaryotic Hsp90 system participates in the refolding of certain thermally denatured polypeptides during the recovery of cells from heat stress (Borkovich et al., 1989). Using firefly luciferase as a model substrate, it was demonstrated that Hsp90 cooperates in this process with Hsp70, Hsp40 (a DnaJ homolog), p60, Hip, and p23 (Schumacher et al., 1994; Schneider et al., 1996). Thus, the Hsp90 complexes formed with the thermally denatured polypeptide resemble those of hormone receptors and protein kinases. Geldanamycin inhibits the Hsp90-mediated refolding of luciferase, both in vitro and in vivo, and, as a result, luciferase is retained in the Hsp90 complex in an unfolded, degradation-sensitive state (Schneider et al., 1996). This shifts the balance from refolding to the proteolytic degradation of the protein (Schneider et al., 1996). Such a mechanism might also explain how, under nonstress conditions, geldanamycin and its homologs cause the degradation of the signaling molecules.

To obtain insights into the function of Hsp90 in these conformational maturation/refolding processes and its inhibition by geldanamycin, we identified the geldanamycin-binding domain of Hsp90 (henceforth Hsp90-GBD), and we determined the crystal structures of this domain and of its complex with geldanamycin.

Results and Discussion

Isolation of the Geldanamycin-Binding Domain of Hsp90

To facilitate the structural study of the geldanamycin-Hsp90 interaction, we first used proteolytic digestion and determined that the bovine Hsp90 contains three structural domains (Figure 1A): an N-terminal domain of approximately 25 kDa, a middle domain of approximately 35 kDa, and a C-terminal domain of approximately 10 kDa. We then assayed the three corresponding recombinant domains of human Hsp90 for geldanamycin binding using gel filtration chromatography to remove excess drug and reverse-phase HPLC to detect the bound drug,

Table 1. Summary of Crystallographic Analysis

Diffraction Data and MIR Analysis

Crystal	Crystal Description	Resolution (Å)	Unique Reflections	Measured Reflections	Coverage (%)	R_{sym} (%)	R_{iso} (%)	Phasing Power	R_c
Native1	I222 (10°C)	2.30	13532	43812	98.0	4.4	—	—	—
Native2	I222 (−160°)	1.65	34516	361958	98.2	3.8	—	—	—
Native3	$P2_1$-Mg (−160°C)	2.20	11381	51794	97.7	3.5	—	—	—
GDM Complex	$P2_1$ (−160°C)	1.90	16906	86335	92.2	2.5	—	—	—
K_2AuCl_4	I222 (10°C)	2.50	10254	49642	94.6	5.7	17	2.43	0.54
K_2PtCl_4	I222 (10°C)	3.20	4713	20129	91.6	5.8	28	1.07	0.83
K_2PtBr_6	I222 (10°C)	3.20	4831	25025	93.1	4.7	22	0.75	0.90
$Sm(OAc)_3$	I222 (10°C)	3.20	4442	16281	86.0	7.1	30	0.65	0.92

Refinement and Analysis of Atomic Models

Crystal	Resolution (Å)	Reflections ($\|F\| > 2\sigma$)	Atoms Modeled (Protein, Water)	R_{cryst}/R_{free} (%, %)	rms Deviations (Bonds [Å], Angles [°], B Factor [Å^2])
Native1	7.0–2.30	12445	1626, 96	16.9, 25.2	0.012, 1.7, 3.2
Native2	6.0–1.65	32524	1626, 335	19.4, 24.4	0.007, 1.6, 3.3
Native3	7.0–2.20	10845	1679, 246	18.9, —	0.010, 1.7, 3.2
GDM Complex	6.0–1.90	16080	1679, 288	18.9, —	0.009, 1.8, 3.2

Coverage is the percentage measured of the total reflections theoretically observable. $R_{sym} = \Sigma_h\Sigma_i \, |I_{h,i} - I_h| \, / \, \Sigma_h\Sigma_i \, I_{h,i}$, where I_h is the mean intensity of the i observations of the unique reflection h. $R_{iso} = \Sigma \, | F_{PH} - F_P| \, / \, \Sigma|F_P|$, where F_P and F_{PH} are the native and derivative structure factor amplitudes, respectively. Phasing power $= [F_{H(calc)}{}^2 \, / \, (F_{PH(obs)} - F_{PH(calc)})^2]^{1/2}$, where $F_{PH(obs)}$ and $F_{PH(calc)}$ are the observed and calculated derivative structure factors, respectively. $R_c = \Sigma||F_{PH} \pm F_p| - F_{H(calc)}| \, / \, \Sigma|F_{PH} \pm F_p|$, for centric reflections only, where $F_{H(calc)}$ is the calculated heavy atom structure factor. Figure of merit $= <\Sigma \, P(\alpha) \exp(i\alpha) \, / \, \Sigma \, P(\alpha)>$, where $P(\alpha)$ is the probability distribution for the phase α. Atoms modeled discounts hydrogen atoms. $R = \Sigma|F_p - F_{calc}| \, / \, \Sigma F_p$, where F_{calc} is the calculated protein structure factor from the atomic model; R_{free} is the R factor calculated using 10% of the reflection data chosen randomly and omitted from the refinement process, whereas R_{cryst} is calculated with the remaining data used in the refinement. rms. bond lengths and angles are the deviations from ideal values; the rms deviation in B factors is calculated between covalently bonded atoms.

and determined that the N-terminal domain, which has the highest sequence conservation among the three domains, binds geldanamycin at an approximately one molar ratio (Figure 1A).

In crystallization experiments, the geldanamycin-binding domain of human Hsp90 (Hsp90-GBD, residues 9–236) produced two distinct crystal forms in which the structure differs by a local conformational change. The geldanamycin–Hsp90-GBD complex crystallized in only one of the two forms. The two apo-Hsp90-GBD structures have been determined at 1.65 and 2.2 Å resolution, respectively, and the structure of the geldanamycin complex at 1.9 Å resolution (Table 1, Figure 1B).

Overall Structure of the Geldanamycin–Hsp90-GBD Complex

The Hsp90-GBD has nine helices and an antiparallel β sheet of eight strands that together fold into an α+β sandwich (Figures 2A–2D). One face of the β sheet is hydrophobic and packs against a layer of five helices; four of these helices (H1, H2, H4, and H9) pack flatly against the β sheet, with their axes parallel to the β strands, while H7 packs against the β sheet at a steeper, almost perpendicular angle. The structure has a second layer of helices that pack on the first layer (H5 and H6), and two smaller helices (H3 and H8) at the periphery of the sandwich (Figures 2A–2D). It is noteworthy that four of the nine helices are of the 3_{10} type and comprise 11.2% of the amino acids, which is significantly higher than the 3.4% average in the protein database (Barlow and Thornton, 1988). At its center, the helical face of the sandwich has a wide opening that extends into the hydrophobic core of the structure and results in a pronounced pocket, about 15 Å deep (Figures 2B–2D). The pocket has the β sheet as its base and three helices and a loop as its walls, and contains residues highly conserved across species (Figure 3). The helical face of the sandwich also has a surface groove that leads into the pocket.

In the complex, the 560 Da geldanamycin adopts a compact conformation and binds inside the pocket, filling all but its deepest portion (Figures 2A–2E). The benzoquinone group of geldanamycin binds near the entrance of the pocket, whereas the ansamycin ring, having dimensions similar to those of a five amino acid polypeptide in a turn conformation, inserts into the pocket. There is extensive, though not complete, surface complementarity between geldanamycin and the pocket, and this allows for a high density of van der Waals contacts. Although hydrogen bond contacts are fewer, there being only five of them, one pair from the geldanamycin carbamate group (Figure 2E) can be reasonably described as one of the most important intermolecular interactions in the complex.

The entrance and width of the pocket are likely regulated by a conformational change, as evidenced by structural and positional changes in three helices and a loop in the two different apo-Hsp90-GBD crystal forms (Table 1). One of the conformations, which is essentially identical to that observed in the crystals of the geldanamycin–Hsp90-GBD complex, has a wide enough entrance to allow geldanamycin binding. The other conformation has a narrower entrance, and it would be incompatible with geldanamycin binding.

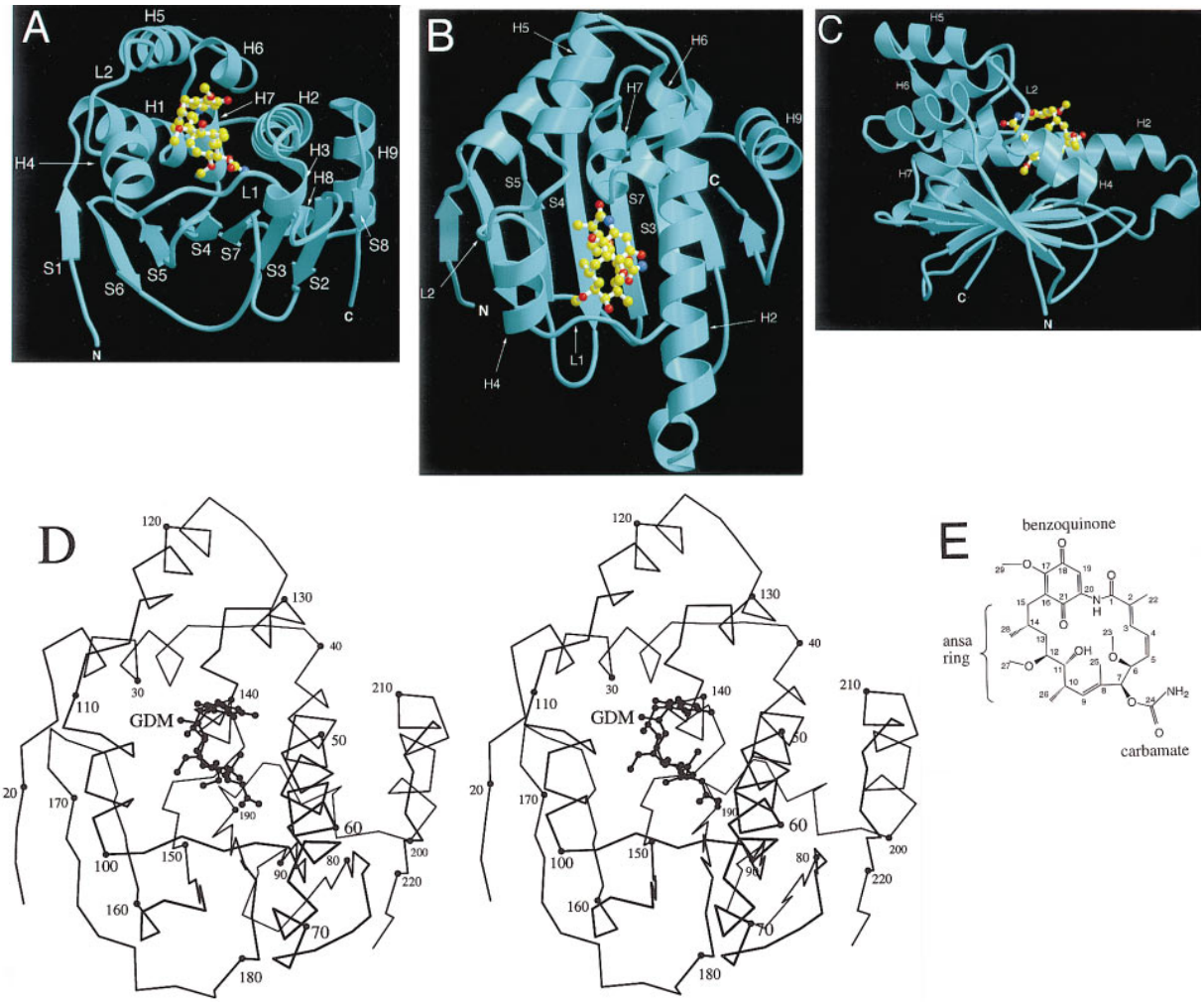

Figure 2. The Hsp90-GBD Is an $\alpha+\beta$ Sandwich with a Deep, Conserved Pocket where Geldanamycin Binds

(A–C) Three approximately orthogonal views of the complex. Geldanamycin atoms are colored yellow for carbon, red for oxygen, and blue for nitrogen. In (A), all secondary structure elements are labeled, whereas in (B) and (C), only those discussed in the text are labeled for clarity. Images were prepared with the programs MOLSCRIPT (Kraulis, 1991) and RASTER3D (Merrit and Murphy, 1994).

(D) Stereo view of the Cα trace of the complex, with every 10th residue numbered and its Cα atom highlighted as a sphere.

(E) Chemical structure of geldanamycin.

Architecture and Properties of the Geldanamycin-Binding Pocket

The pocket can be described as a flat-bottomed cone: it is about 15 Å deep, 12 Å in diameter near its entrance, 8 Å midway down, and wide enough at the bottom to hold three water molecules (Figure 4A). The bottom of the pocket is formed by the central portion of the antiparallel β sheet (strands S3, S4, and S7), and the walls by the H2, H4, and H7 helices and the L1 loop (Figure 3). The pocket is deepest by the H7 helix, which packs at an almost perpendicular angle to the β sheet bottom, and is shallowest by the L1 loop. The pocket is of mixed hydrophobic and polar character, with roughly half of the 17 amino acids lining its interior being hydrophobic, a quarter polar, and a quarter charged (these residues are Leu48, Asn51, Asp54, Ala55, Lys58, Ile91, Asp93, Ile96, Gly97, Met98, Asn106, Leu107, Lys112, Gly135, Phe138, Val150, Thr184, and Val186; Figure 3). Although the pocket becomes increasingly hydrophobic toward the bottom, it retains one charged and one polar residue at its deepest portion (Asp93 and Thr184 from the β sheet).

The Hsp90-GBD domain is highly conserved across species, with 43% of its residues identical in the Escherichia coli Hsp90 homolog. The structure reveals that the conserved residues are not distributed homogeneously on the structure, but instead show a striking tendency to cluster in and around the pocket, with 82% of the residues lining the interior of the pocket being invariant from E. coli to humans (Figures 3 and 4B). This identifies the pocket as holding the key to understanding the function of this domain. Of particular interest is Asp93, because it is at the pocket bottom in an otherwise mostly hydrophobic environment, and because it is conserved in all known Hsp90 homologs from 35 species.

Supporting a functional significance for this pocket are mutations in the yeast homolog of Hsp90 (Hsp82) that result in either temperature-sensitive or reduced activity phenotypes (Bohen and Yamamoto, 1993; Sullivan and Toft, 1993; Kimura et al., 1994; Nathan and

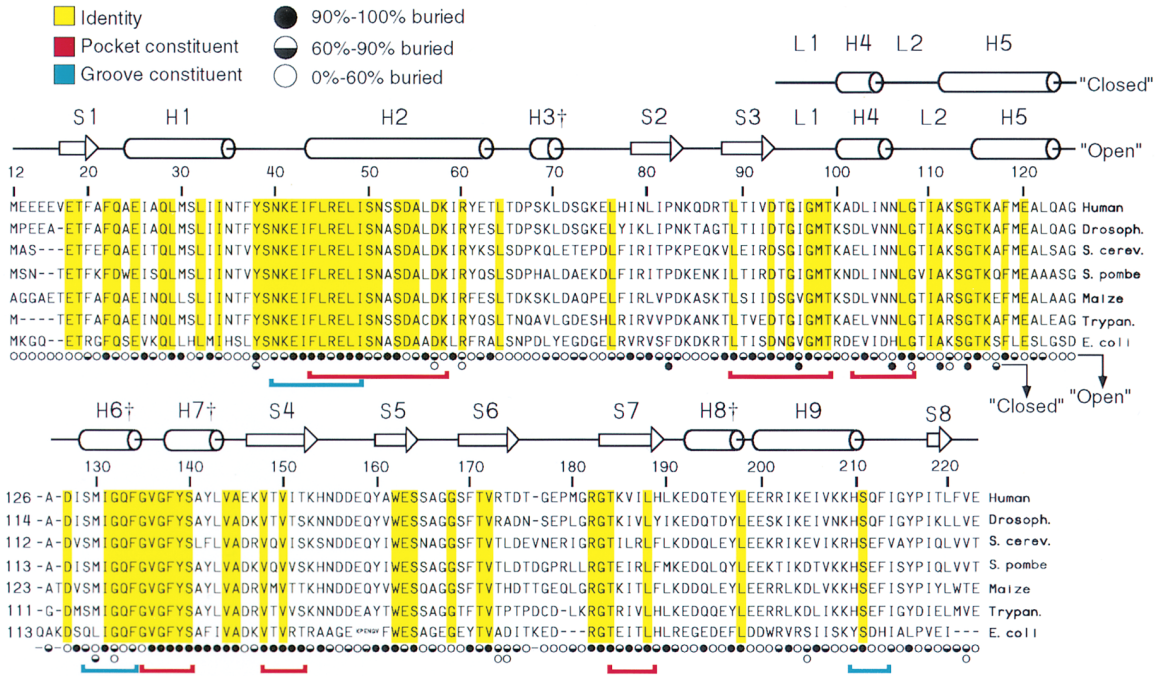

Figure 3. Alignment of Hsp90-GBD Sequences from Several Diverse Species

Secondary structure elements for the $P2_1$ (open) form are indicated above the sequence together with the changes observed in the I222 (closed) form. Invariant residues are highlighted in yellow, residues that make up the pocket are underlined in red, and residues that make up the surface groove are underlined in blue. Residue solvent accessibilities are indicated with circles (open, half-closed, or closed). The dagger symbol indicates 3_{10} helices.

Lindquist, 1995), as well as a mutation in the Drosophila Hsp90 (Hsp83) that impairs signaling by the Sevenless receptor tyrosine kinase (Cutforth and Rubin, 1994). These mutations map either in the pocket (Ala55Val, Gly95Ser, Gly183Asp) or in the immediate vicinity of the pocket (Thr36Asn, Ser50Leu, Ala111Thr, Thr115Ile), and

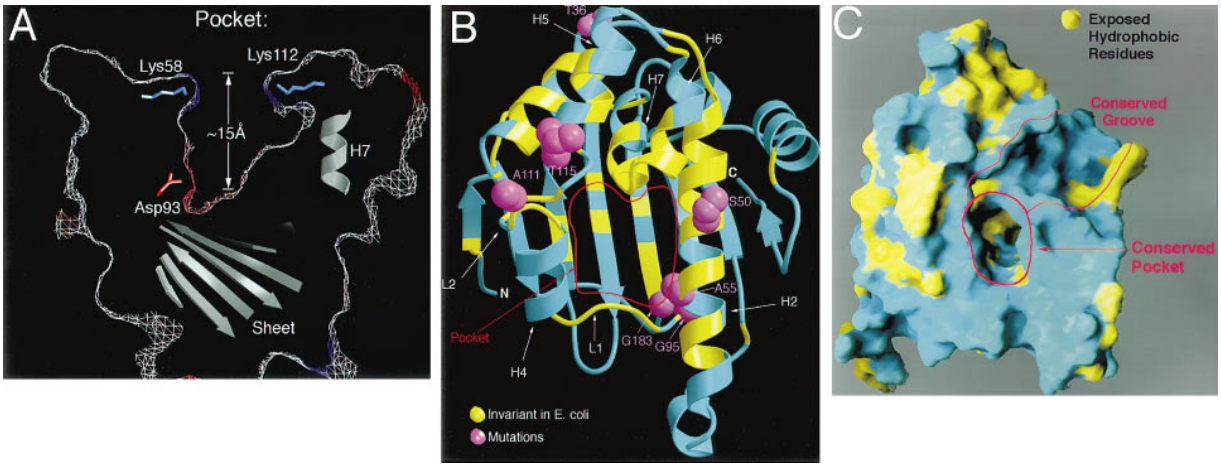

Figure 4. The Hsp90-GBD Has a Conserved Pocket That Is 15 Å Deep

(A) A thin slice of the Hsp90-GBD molecular surface, depicted as a white net, stressing the pocket dimensions. Red indicates surface portions with a negative electrostatic potential, and blue those with a positive potential. The pocket is mostly polar at its entrance (Lys58 and Lys112 are shown), and it becomes predominantly hydrophobic near the bottom, except for Asp93. The approximate locations of the β sheet and of the H7 helix are indicated; the H2 helix would be approximately above the plane of the figure, whereas the H4 helix would be below. This image was prepared with the program GRASP (Nicholls et al., 1991).

(B) Yellow highlights the positions of residues invariant in the E. coli Hsp90 homolog; magenta highlights residues, shown in space filling representation, where either temperature-sensitive or inactivating mutations map.

(C) Surface representation indicating the pocket and groove. Also indicated, in yellow, are several patches of exposed hydrophobic amino acids in the vicinity of the pocket and groove. These hydrophobic residues are: Phe213 to the right of the groove in this view; Ala117, Ala121, Ala124, Ala126, Met130, and Phe134 to the left of the groove; and Phe20, Ile104, Ala111, and Ile112 to the left of the pocket (prepared with the program GRASP).

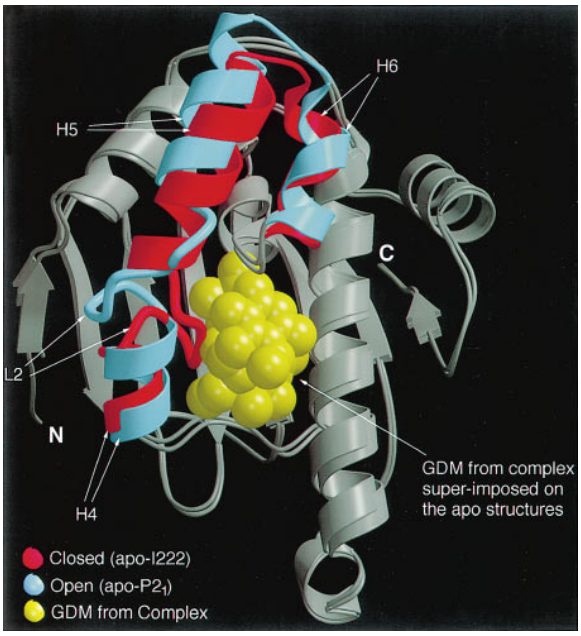

Figure 5. A Conformational Change Alters the Size and Accessibility of the Pocket in the Absence of Geldanamycin

The secondary structural elements that undergo positional and conformational changes are shown in red for the I222 (closed) and in cyan for the $P2_1$ (open) apo-Hsp90-GBD crystal forms. Geldanamycin, in space-filling representation, is superimposed on the figure to stress the effects that the conformational change has on the pocket size.

the structure suggests that most of these mutations would disrupt the structural integrity of the pocket (Figures 3 and 4B).

Leading to the pocket, there is a surface groove formed by the H6 and H9 helices on the sides, and the H2 helix at its bottom (Figure 4C). Its shape is not as pronounced as the pocket, being shallower (about 7–8 Å), broader (about 15 Å), and mostly polar. This groove is conserved, although not as well as the pocket, with 73% of the residues lining its concave surface identical in the E. coli homolog (these residues are Asn40, Glu42, Ile43, Arg46, Glu47, Ser50, Ser129, Gln133, His210, Ser211, and Ile214; Figure 3). Since many of these residues are polar or charged, without any significant roles in the structural integrity of this domain, their conservation suggests that the groove may participate in intermolecular interactions important for Hsp90 function.

Conformational Change Alters the Size and Accessibility of the Pocket

An approximately 35 amino acid region of the Hsp90-GBD structure, consisting of the H4-L2-H5-H6 secondary structure elements (residues 100–134), has two different conformations in the two different Apo-Hsp90-GBD crystal forms (Table 1, Figures 3 and 5). We have termed these the "open" and "closed" conformations because they result in different pocket size and accessibility, with only the open conformation being compatible with geldanamycin binding.

At the center of the open-to-closed conformational change is a displacement of the L2 loop into the pocket by more than 9 Å (Cα–Cα distance), whereupon the L2 loop replaces the H4 helix as one of the pocket walls. The motion of the L2 loop is facilitated by portions of the H4 and H5 helices undergoing helix-to-coil and coil-to-helix transitions, respectively (Figures 3 and 5). The H4 and H5 helices also are displaced, by up to 6 Å. The functional consequence of this conformational change is that the L2 loop acts as a gate that constricts the pocket entrance from a width of 12 Å to 8 Å (Figure 5).

These two alternate conformations have clear electron density in their respective crystal forms and are associated with well-packed side chain arrangements (Figure 3). It is conceivable that this conformational change in vitro may mimic a process that occurs in vivo and may be involved in the regulation or functioning of the pocket. Supporting an in vivo role for the closed conformation is the Ala111Thr mutation on the L2 loop that results in a temperature-sensitive phenotype in yeast (Kimura et al., 1994). This mutation would disrupt the closed conformation structure where Ala111 is fully buried and participates in the hydrophobic packing of the loop, but not the open conformation structure where Ala111 is fully solvent exposed with no apparent structure-stabilizing role.

Structure of Geldanamycin

Geldanamycin consists of a closed ansa ring with a planar benzoquinone embedded in it (Figure 2E). The ansa ring is sterically hindered because (1) its backbone consists of a planar amide and three carbon-carbon double bonds (two of them arranged in a 1,3 diene), and (2) of its sixteen backbone atoms, nine carry nonhydrogen substituents: a carbonyl, a carbamate (–$OC(O)NH_2$), a hydroxyl, two methoxy, and four methyl groups (Figure 2E).

Hsp90-bound geldanamycin is highly compact and internally well packed (overall dimensions of about 9 × 9 × 9 Å). Its ansa ring is folded over the benzoquinone, forming a C-clamp-like structure, with the benzoquinone forming the top of the (C) and the ansa ring forming the stem and bottom of the (C) (Figure 6A). Two of the methyl groups from the ansa ring are centrally positioned to maximize intramolecular van der Waals contacts: the C25 methyl group from the tip of the ansa ring packs with the benzoquinone, thus bridging the top and bottom halves of the (C), and the C28 methyl group packs with the diene carbon atoms, bridging the two sides of the ansa ring (Figure 6A).

This compact conformation differs from those observed with free geldanamycin (Rinehart and Shield, 1976) or herbimycin (Furusaki et al., 1980), which crystallize from organic solvents in significantly more open, extended conformations. The differences are likely due, in part, to the loss of coplanarity between the amide group and the benzoquinone in Hsp90-bound geldanamycin, as well as to the differences in the crystallization solvents.

Geldanamycin–Hsp90 Contacts

The tip of the geldanamycin ansa ring (bottom of [C]), which has the carbamate, C23 methoxy, and C25 and

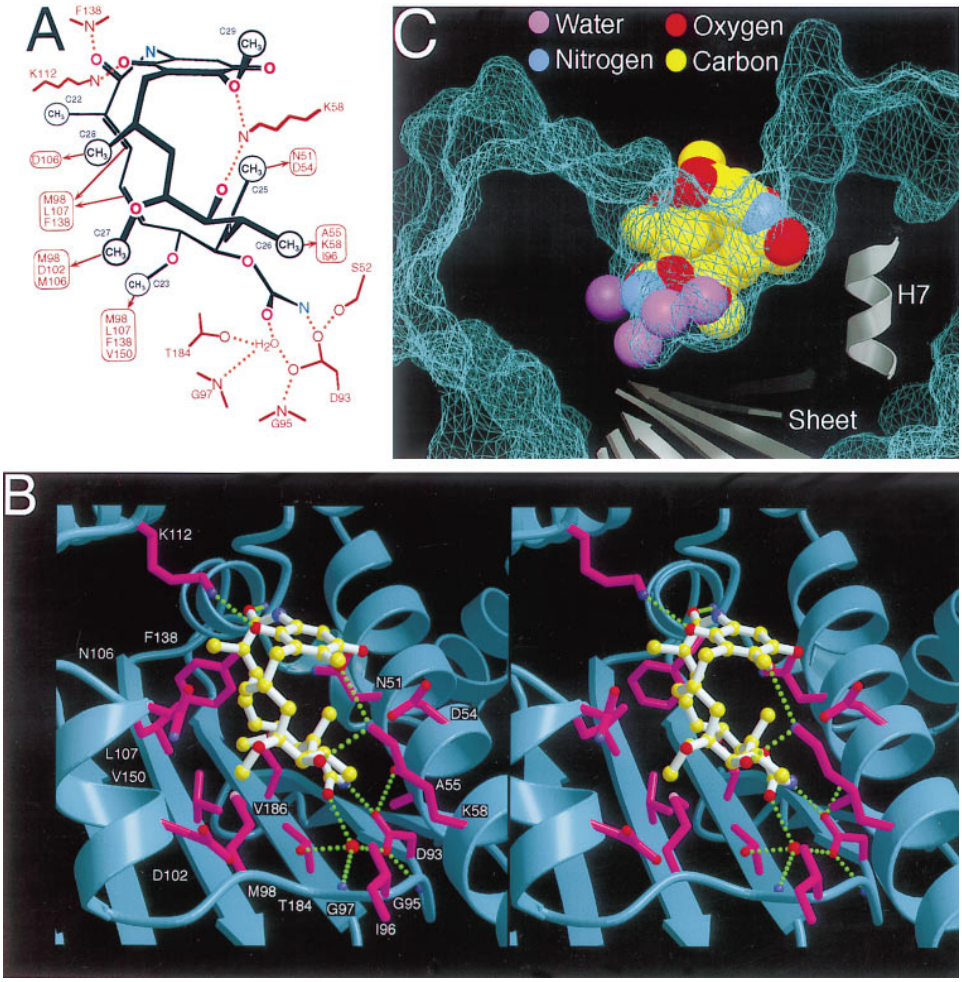

Figure 6. Hsp90-Bound Geldanamycin Adopts a Compact Conformation Reminiscent of the Letter (C) and Binds Hsp90 by Inserting the Tip of Its Ansa Ring inside the Pocket

(A) Diagram of the bound geldanamycin conformation summarizing the hydrogen bond (dotted lines) and van der Waals (arrows) contacts it makes with Hsp90 residues, colored brown. The oxygen atoms of geldanamycin are shown in red, nitrogen atoms in blue, and methyl groups as closed circles; the remaining carbon atoms are not explicitly shown.

(B) Stereo view of the geldanamycin–Hsp90-GBD interactions. Geldanamycin is colored as in Figure 2A, and Hsp90 residues that make up the pocket are colored magenta. Hydrogen bonds are indicated by green dotted lines, and the water molecule that bridges the geldanamycin carbamate group with Asp93 is shown as a red sphere.

(C) Geldanamycin, in space-filling representation, adopts a structure that is, overall, complementary to the pocket, shown as a blue molecular surface net. Although the fit is extensive, there remains a buried cavity at the interface with three trapped water molecules in it (colored magenta), while a fourth water molecule hydrogen bonds with the carbamate group and Asp93. The reduced complementarity near the pocket entrance is evident as gaps between the geldanamycin atoms and the Hsp90-GBD surface. Orientation is similar to that of Figure 4A.

C26 methyl group substituents, binds near the bottom of the Hsp90 pocket and makes a high density of van der Waals contacts, whereas the benzoquinone (top of [C]) is positioned near the entrance of the pocket and makes only a few contacts (Figures 6A and 6B). There is extensive surface complementarity between the compact geldanamycin structure and the pocket, as attested by the fact that a remarkable 85% of the surface area of geldanamycin is buried in the complex (609 Å^2 out of 719 Å^2).

The most critical portion of the interface is likely to be a hydrogen bond network between the geldanamycin carbamate group and the Asp93 side chain from Hsp90, which are buried at the pocket bottom in an otherwise mostly hydrophobic environment. The carbamate amino group makes a hydrogen bond to one of the Asp93 side chain oxygen atoms, and its carbonyl oxygen atom makes a water-bridged hydrogen bond with the other Asp93 side chain oxygen atom (Figures 6A and 6B). The Asp93 side chain, which has an identical conformation in the Apo-Hsp90 structures, also hydrogen bonds to the Ser52 OH and the backbone amide of residue 95. This hydrogen bond network is buried about 10 Å away from the nearest solvent surface, and the low dielectric constant of this environment would significantly increase the coulombic attraction due to the partial charges. The importance of this hydrogen bond network is supported by structure activity studies demonstrating

that the removal of the carbamate group, or the attachment of additional atoms to it, completely abolished geldanamycin activity (Schnur et al., 1995b).

At the tip of the ansa ring, the carbamate group contact is flanked by the C23 methoxy and C25 and C26 methyl groups making high density van der Waals contacts with the bottom and sides of the pocket (Figures 6A and 6B). Although the surface complementarity at the pocket bottom is extensive, there remains a buried cavity filled with three water molecules near the C23 methoxy and the carbamate groups (Figure 6C). It is conceivable that the cellular substrates of Hsp90 can fill this cavity as well. Modifications to this portion of geldanamycin, for example by adding to the C23 position a group of 4–6 nonhydrogen atoms, could increase the steric and hydrogen bond complementarity and may yield derivatives with increased affinity for Hsp90.

Halfway between the pocket bottom and the surface, the widening of the pocket causes a decrease in the complementarity and contact density, although the fit is still adequate to exclude bulk solvent (Figure 6C). In this region, the diene and the C27 methoxy groups make van der Waals contacts, and the O5 hydroxyl group makes a hydrogen bond contact with Lys58 (Figures 6A and 6B). As we get closer to the surface, the contact density decreases further. In this region, the C28 methyl group appears to be in an overall unfavorable environment, being within van der Waals contact distance to a backbone carbonyl oxygen atom and a partially buried water molecule (Figures 6A and 6B). The loose fit in this region, both sterically and electrostatically, points to a potential for a significant improvement of the affinity of geldanamycin for Hsp90 (Figure 6C).

At the pocket entrance, the carbonyl oxygen atom of the ansa ring makes a hydrogen bond to a backbone amide (Phe138) at the N-terminal portion of the H7 helix (Figures 6A and 6B). The benzoquinone, which is at the pocket entrance with one face solvent-exposed, makes only a few contacts, and these are primarily solvent-exposed hydrogen bonds made to long lysine chains: one of the benzoquinone oxygen atoms hydrogen bonds with Lys112, and the C29 methoxy group oxygen atom makes a long-distance (3.5 Å) hydrogen bond with Lys58.

Geldanamycin Derivatives

Among the naturally occurring homologs, geldanamycin is the most potent. Compared to herbimycin, for example, geldanamycin is more potent by a factor of about four in achieving a 50% reduction (IC_{50}) of erbB-2 kinase activity in human SKBr3 breast cancer cells (Miller et al., 1994). The structure suggests that this may be due to the hydrogen bond that the C29 methoxy oxygen atom of geldanamycin makes with Lys58, because herbimycin does not have the C29 methoxy group.

Among the published synthetic derivatives (Schnur et al., 1995a, 1995b), the highest potency, reflecting an improvement in the IC_{50} of a factor of 4–5, was achieved by an amino group substitution at the C17 position of the benzoquinone (Schnur et al., 1995a). It was proposed that this and several related substitutions at the C17 position improved cellular activity indirectly, by stabilizing the quinone form over the reduced hydroquinone (Schnur et al., 1995a). The structure supports this hypothesis, as this position is highly solvent exposed in the complex and is a poor candidate for additional Hsp90 contacts.

Overall, however, most modifications decreased or eliminated activity (Schnur et al., 1995a, 1995b). The maintenance of the carbamate group and of the closed, cyclic nature of the ansa ring proved necessary for activity (Schnur et al., 1995b), consistent with the extended hydrogen bond network that the carbamate group makes and with the importance of a closed cyclic ring in limiting conformational flexibility, respectively. Modifications at other positions either had little effect or reduced the activity of geldanamycin in line with space considerations revealed by the crystal structure. For example, additions of small groups to the amide nitrogen and to the C19 position of the benzoquinone, which are juxtaposed in a partially solvent-exposed region of the complex, were tolerated (Schnur et al., 1995a, 1995b), whereas bulky substituents at these positions reduced or eliminated activity (Schnur et al., 1995b).

Our crystal structure suggests modifications, such as those at the C23 methoxy and C22 methyl groups discussed earlier, that could improve the steric and hydrogen bond complementarity between geldanamycin and Hsp90 and could thus provide analogs with increased Hsp90 affinity (a total synthesis of geldanamycin has recently been reported [Miller, 1995]). In addition, by identifying which modifications are compatible with Hsp90 binding, the structure should also help with the improvement of geldanamycin's low plasma half-life (Supko et al., 1995) and other pharmacological properties as well.

Implications for Understanding Hsp90 Function

The pocket is best considered as a substrate-binding site, for there are extensive similarities between the pocket and a typical enzyme active site, though no covalent chemistry is implied by the similarities. We note that: (1) the pocket has adequate space and hydrophobic content, and is adequately shielded from bulk solvent to tightly bind substrates of a few hundred daltons; (2) there is a nonuniform electrostatic distribution resulting from an aspartic acid at the otherwise hydrophobic bottom of the pocket; (3) the shape and size of the pocket entrance is likely to be regulated by a conformational change; (4) the geldanamycin-binding domain of Hsp90 is the best conserved among its three structural domains, and within this domain, the conserved residues cluster in and around the pocket; (5) mutations that inactivate Hsp90 map in and around the pocket; and, finally, (6) the geldanamycin inhibitor of Hsp90 function binds inside this pocket.

Assuming that the Hsp90 pocket is a substrate binding site, it can then directly follow that its substrate is the protein, or more precisely, a segment of the protein, whose conformational maturation/refolding is mediated by the Hsp90 chaperone system. This pocket-polypeptide association is likely to occur as a late step in the reaction pathway because Hsp70, which is present in all of the early Hsp90 complexes (Smith, 1993; Smith et

al., 1995; Dittmar et al., 1996; Johnson et al., 1996), can bind unfolded proteins (Flynn et al., 1991; Zhu et al., 1996) and is thus the likely initial recruiter of the unfolded polypeptide to the Hsp90 complex. That a polypeptide portion is the substrate for the pocket is supported by the ability of the endoplasmic reticulum homolog, GP96, to associate with a specific viral peptide, though it is not yet known with which domain of GP96 this peptide is associated (Nieland et al., 1996).

Further support is provided by the general similarities between the geldanamycin ansa ring and a peptide. A five amino acid polypeptide in a turn conformation could closely trace the geldanamycin ansa ring backbone, with its amino acid side chains broadly corresponding to the carbamate, methyl, and methoxy groups of geldanamycin (Figure 7). Furthermore, and intended only as an example, steric and hydrogen bond complementarity considerations suggest that a tryptophan amino acid could be accommodated at the polypeptide position corresponding to that of the geldanamycin carbamate group (Figure 7). The tryptophan indole amino group could donate a hydrogen bond to Asp93, in a manner analogous to that of the carbamate amino group, perhaps explaining why Asp93 is conserved, and the hydrophobic portion of the tryptophan could fill the buried cavity that is now occupied by water molecules in the geldanamycin complex (Figure 7). In this region, backbone amide groups, as well as other hydrogen bond donor amino acids, could also satisfy the hydrogen bond potential of Asp93, although they may not have as good of a fit as a tryptophan in the buried cavity.

It is conceivable that the pocket binds a family of related polypeptide sequences, and this could explain the conservation of the pocket residues, because a large family of peptide sequences, in contrast to a single sequence, could not coevolve with amino acid changes in the pocket. This has precedence in the Hsp70 chaperone, which has a peptide-binding channel highly conserved between E. coli and humans (Zhu et al., 1996), and binds unfolded proteins by interacting with seven-residue segments, having exposed hydrophobic amino acids at their central positions (Flynn et al., 1991; Zhu et al., 1996).

A model in which the polypeptide substrate binds in the pocket along the reaction pathway would be supported by the observation that geldanamycin causes the dissociation of the v-src–Hsp90 complex in transformed cells (Whitesell et al., 1994). Also consistent are observations from the in vitro conformational maturation of the steroid receptors. In this reaction, a transient complex of the receptor that includes Hsp90, Hsp70, and several other cofactors is in equilibrium with the hormone-responsive state of the receptor, which is bound to Hsp90, p23, and an immunophilin (Smith et al., 1995; Dittmar et al., 1996; Nair et al., 1996). Geldanamycin blocks the formation of the latter complex, consistent with receptor–pocket interactions being required to either arrive at or to maintain the hormone-responsive state of the receptor (Smith et al., 1995; Nair et al., 1996). In principle, the interruption of this reaction by geldanamycin can be interpreted in other ways, for example, to mean that geldanamycin directly competes with p23 (Smith et al., 1995) binding to the pocket. This is possible; however, we note that: (1) it is unlikely that such an unusual pocket would have evolved to bind a protein cofactor; (2) p23 and the pocket could have coevolved resulting in far lesser sequence conservation at the pocket; and (3) E. coli and lower eukaryotes do not seem to have p23, at least not one that is as conserved as the Hsp90-GBD.

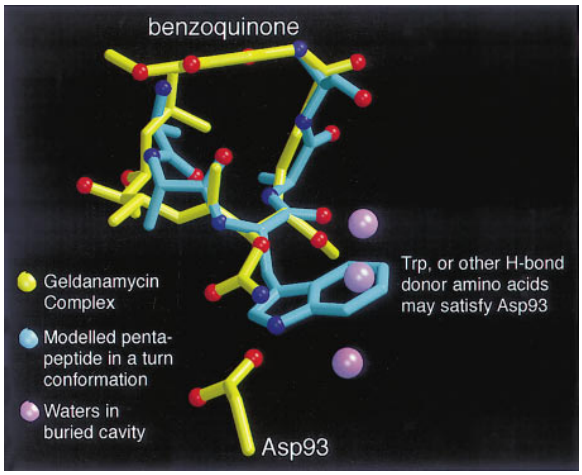

Figure 7. The Geldanamycin Ansa Ring Adopts a Structure Reminiscent of a Pentapeptide in a Turn Conformation

Geldanamycin and Asp93 of Hsp90 are in yellow, the buried water molecules at the geldanamycin–Hsp90-GBD interface are in magenta, and the modeled polypeptide is in cyan. Red and blue indicate oxygen and nitrogen atoms, respectively. A tryptophan at the peptide position corresponding to that of the carbamate group in geldanamycin could donate a hydrogen bond to Asp93 of Hsp90 and also pack in the hydrophobic cavity now occupied by the three water molecules. Backbone amide groups and several other amino acids could also hydrogen bond to Asp93, but their fit in the pocket would not be as good as that of a Trp.

On the other hand, the isolation of complexes of heat-denatured luciferase and of Raf with Hsp90 in the presence of geldanamycin (Schneider et al., 1996) at first appears to be inconsistent with the pocket binding these substrates. It is conceivable, however, that Hsp90 contains additional polypeptide-interacting sites that are not blocked by geldanamycin and that act at an earlier stage. These additional sites can be either within its geldanamycin-binding domain (for example, the conserved surface groove) or in the rest of the 732 residue protein. Alternatively, the observed association of geldanamycin-bound Hsp90 with the protein substrate may be indirect, since these complexes contain several other protein cofactors, such as Hsp70, which may contribute to polypeptide binding (Bose et al., 1996; Duina et al., 1996; Freeman et al., 1996; Schneider et al., 1996). In any case, geldanamycin blocks the refolding of the heat-denatured Raf and luciferase substrates, and this ultimately results in their degradation (Schneider et al., 1996).

The crystal structure of the Hsp90-GBD reveals a pocket whose properties indicate that it is a likely binding site for the polypeptide substrate. That geldanamycin, by binding in this pocket, inhibits the Hsp90-catalyzed conformational reaction both in vitro and in

vivo strongly argues that the pocket–substrate interaction is a required step in this reaction. The crystal structure of this pocket, as well as that of the geldanamycin–pocket complex, also provides a rational basis for the development of geldanamycin derivatives with improved antitumor activity.

Experimental Procedures

Identification of the Geldanamycin-Binding Domain of Hsp90

Bovine Hsp90, prepared from brains as described (Koyasu et al., 1986), was digested by subtilisin, and the products were delineated by N-terminal sequencing and mass spectroscopy. The C terminus of the middle domain is estimated based on its mobility in SDS–PAGE because this fragment was not amenable to mass spectroscopic analysis. The corresponding fragments of human Hsp90 were overexpressed in E. coli using the pET3d vector (Novagen), and the recombinant domains were purified by ion exchange and gel filtration chromatography.

Crystallization and Data Collection

For crystallization, the recombinant human Hsp90-GBD (residues 9–236) was concentrated by ultrafiltration to 30 mg/ml and was further purified by gel filtration chromatography. The geldanamycin–Hsp90-GBD complex was prepared by mixing the purified protein with a 2-fold molar excess of geldanamycin (GIBCO-BRL), fractionation by gel filtration, and concentration by ultrafiltration to 17 mg/ml. Two crystal forms were grown at 7°C using the method of hanging-drop vapor diffusion. One form (Native1 and Native2 in Table 1) grew from a buffer of 0.1 M sodium cacodylate (pH 6.5), 0.2 M ammonium sulfate, and 30 percent w/v polyethylene glycol 8000 (PEG8000) in spacegroup I222 with a = 66.2 Å, b = 90.1 Å, c = 101.2 Å. Another form (Native3) grew from 0.1 M Tris–HCl, 0.2 M magnesium chloride, and 30% PEG4000 (pH 8.5) in spacegroup $P2_1$ with a = 53.4 Å, b = 44.1 Å, c = 54.0 Å, β = 115.7°. Crystals of the geldanamycin–Hsp90-GBD complex (GDM complex in Table 1) grew from a buffer of 0.1 M Tris–HCl, 0.2 M sodium acetate, and 33% w/v PEG4000 (pH 8.5) in spacegroup $P2_1$, with a = 53.7 Å, b = 44.3 Å, c = 54.6 Å, β = 116.1° (same space group as Native3), and had a violet coloring. Data were collected on an R-AXISIIC imaging plate detector mounted on a Rigaku 200HB X-ray generator, at 10°C for Native1 and the derivatized crystals. For the other data sets, crystals were flash frozen at −160.0°C either in 30% PEG8000 and 20% glycerol (Native2) or in 35% PEG4000 (Native3 and GDM complex).

Structure Determination and Refinement

The heavy atom derivatives were prepared by soaking I222 form crystals in a buffer of 75 mM sodium cacodylate, 0.15 M ammonium sulfate, and 40% PEG8000 (pH 6.5) containing one of the following heavy atom solutions: saturated K_2AuCl_4 for 52 hr, 20 mM K_2PtCl_4 for 24 hr, and 20 mM K_2PtBr_6 for 60 hr. An additional derivative was obtained in 5 mM sodium cacodylate, 250 mM NaCl, 33% PEG8000 with 0.5 mM $Sm(OAc)_3$ (pH 7.0) for 14 hr. The multiple isomorphous replacement (MIR) analysis was performed using the CCP4 suite of programs (Collaborative Computational Project, Number 4, 1994). MIR phases had a mean figure of merit of 0.66 to 3.2 Å and were improved by solvent flattening and histogram matching. The initial model building was followed by several cycles of refinement with the program X-PLOR (Brunger, 1991) and by weighted combination between model phases and MIR phases, and this allowed for a continuous trace of residues 17–223. Amino acids 9–16 and 224–236 in the I222 form were not visible in the electron density maps and are presumed to be disordered. The $P2_1$ crystal form was solved by molecular replacement with X-PLOR. Difference density maps revealed that amino acids 105–132, and especially 105–112, had undergone significant structural rearrangement compared to the I222 form. In the crystals of the complex, geldanamycin was prominent in the early difference electron density maps and was built using the crystal structure of free herbimycin (Furusaki et al., 1980) as a starting point. In addition, in both $P2_1$ forms, the amino-terminal residues 11–16 were visible and modeled, whereas two solvent-exposed loops, 121–130 and 212–214, became partially disordered relative to the I222 crystals. Residues in all models were in the allowed regions of the Ramachandran plot, with 89% or more in the most favored regions. It is not clear what causes the conformational change in vitro; the L2 loop, which changes the most, is not involved in any significant crystal-packing contacts, though the H5 and H6 helices are in both crystal forms. In addition to magnesium and geldanamycin, the growth of the $P2_1$ form can be induced by acidic pH as well.

Acknowledgments

We thank S. Geromanos and H. Erdjument-Bromage of the Sloan-Kettering Microchemistry Facility for NH_2-terminal sequence and mass spectroscopic analyses, and O. Ouerfelli for helpful discussions about geldanamycin. This research was supported by the National Institutes of Health, the Pew Charitable Trusts, the Arnold and Mabel Beckman Foundation, the Dewitt Wallace Foundation, and the Samuel and May Rudin Foundation. Correspondence and requests for materials should be addressed to N. P. P. (nikola@xray2.mskcc.org). Coordinates have been deposited in the Brookhaven Protein Data Bank (ID codes 1YER, 1YES, and 1YET).

Received February 27, 1997; revised March 17, 1997.

References

Aligue, R., Akhavan-Niak, H., and Russell, P. (1994). A role for Hsp90 in cell cycle control: Wee1 tyrosine kinase activity requires interaction with Hsp90. EMBO J. *13*, 6099–6106.

Barlow, D.J., and Thornton, J.M. (1988). Helix geometry in proteins. J. Mol. Biol. *201*, 601–619.

Bohen, S.P., and Yamamoto, K.R. (1994). The Biology of Heat Shock Proteins and Molecular Chaperones, R.I. Morimoto, A. Tissieres and C. Georgopoulos, eds. (Cold Spring Harbor, NY: Cold Spring Harbor Laboratory Press).

Bohen, S.P., and Yamamoto, K.R. (1993). Isolation of Hsp90 mutants by screening for decreased steroid receptor function. Proc. Natl. Acad. Sci. USA *90*, 11424–11428.

Borkovich, K.A., Farrelly, F.W., Finkelstein, D.B., Taulien, J., and Lindquist, S. (1989). hsp82 is an essential protein that is required in higher concentrations for growth of cells at higher temperatures. Mol. Cell. Biol. *9*, 3919–3930.

Bose, S., Weikl, T., Bugl, H., and Buchner, J. (1996). Chaperone function of hsp90-associated proteins. Science *274*, 1715–1717.

Bouchard, L., Lamarre, L., and Tremblay, P.J. (1989). Stochastic appearance of mammary tumors in transgenic mice carrying the MMTV/c-*neu* oncogene. Cell *57*, 931–940.

Bresnick, E.H., Dalman, F.C., Sanchez, E.R., and Pratt, W.B. (1989). Evidence that the 90-kDa heat shock protein is necessary for the steroid binding conformation of the L cell glucocorticoid receptor. J. Biol. Chem. *264*, 4992–4997.

Brunger, A.T. (1991). X-PLOR, a system for X-ray crystallography and NMR, Version 3.1, Yale University. (New Haven, CT: Yale Univ. Press).

Chavany, C., Mimnaugh, E., Miller, P., Bitton, R., Nguyen, P., Trepel, J., Whitesell, L., Schnur, R., Moyer, J.D., and Neckers, L. (1996). p185(erbB2) binds to GRP94 in vivo—dissociation of the p185(erbB2)/GRP94 heterocomplex by benzoquinone ansamycins precedes depletion of p185(erbB2). J. Biol. Chem. *271*, 4974–4977.

Collaborative Computational Project, Number 4. (1994). The CCP4 suite: programs for protein crystallography. Acta Cryst. *D50*, 760–763.

Cutforth, T., and Rubin, G.M. (1994). Mutations in *Hsp83* and *cdc37* impair signaling by the Sevenless receptor tyrosine kinase in Drosophila. Cell *77*, 1027–1036.

DeBoer, C., Meulman, P.A., Wnuk, R.J., and Peterson, D.H. (1970). Geldanamycin, a new antibiotic. J. Antibiot. (Tokyo) *23*, 442–447.

Dittmar, K.D., Hutchison, K.A., Owens-Grillo, J.K., and Pratt, W.B.

(1996). Reconstitution of the steroid receptor–hsp90 heterocomplex assembly system of rabbit reticulocyte lysate. J. Biol. Chem. *271*, 12833–12839.

Duina, A.A., Chang, H.J., Marsh, J.A., Lindquist, S., and Gaber, R.F. (1996). A cyclophilin function in hsp90-dependent signal transduction. Science *274*, 1713–1715.

Flynn, G.C., Pohl, J., Flocco, M.T., and Rothman, J.E. (1991). Peptide-binding specificity of the molecular chaperone BiP. Nature *353*, 726–730.

Freeman, B.C., and Morimoto, R.I. (1996). The human cytosolic molecular chaperones hsp90, hsp70 (hsc70) and hdj-1 have distinct roles in recognition of a non-native protein and protein refolding. EMBO J. *15*, 2969–2979.

Freeman, B.C., Toft, D.O., and Morimoto, R.I. (1996). Molecular chaperone machines: chaperone activities of the cyclophilin cyp-40 and the steroid aporeceptor–associated protein p23. Science *274*, 1718–1720.

Furusaki, A., Matsumoto, T., Nakagawa, A., and Omura, S. (1980). Herbimycin A: an ansamycin antibiotic; X-ray crystal structure. J. Antibiot. (Tokyo) *33*, 781–782.

Hartson, S.D., and Matts, R.L. (1994). Association of Hsp90 with cellular Src-family kinases in a cell-free system correlates with altered kinase structure and function. Biochemistry *33*, 8912–8920.

Hunter, T., and Pines, J. (1994). Cyclins and cancer II: cyclin D and CDK inhibitors come of age. Cell *79*, 573–582.

Isaacs, J.T., and Coffey, D.S. (1979). Androgenic control of prostatic growth: regulation of steroid levels. UICC Monograph (Prostatic Cancer) *48*, 112–122.

Jakob, U., and Buchner, J. (1994). Assisting spontaneity: the role of Hsp90 and small Hsps as molecular chaperones. Trends Biochem. Sci. *19*, 205–211.

Johnson, J., Corbisier, R., Stensgard, B., and Toft, D. (1996). The involvement of p23, hsp90, and immunophilins in the assembly of progesterone receptor complexes. J. Steroid Biochem. Mol. Biol. *56*, 31–37.

June, C.H., Fletcher, M.C., Ledbetter, J.A., Schieven, G.L., Siegel, J.N., Phillips, A.F., and Samelson, L.E. (1990). Inhibition of tyrosine phosphorylation prevents T-cell receptor–mediated signal transduction. Proc. Natl. Acad. Sci. USA *87*, 7722–7726.

Kimura, Y., Matsumoto, S., and Yahara, I. (1994). Temperature-sensitive mutants of hsp82 of the budding yeast Saccharomyces cerevisiae. Mol. Gen. Genet. *242*, 517–527.

Koyasu, S., Nishida, E., Kadowaki, T., Matsuzaki, F., Iida, K., Harada, F., Kasuga, M., Sakai, H., and Yahara, I. (1986). Two mammalian heat shock proteins, HSP90 and HSP100, are actin-binding proteins. Proc. Natl. Acad. Sci. USA *83*, 8054–8058.

Kraulis, P.J. (1991). Molscript: a program to produce both detailed and schematic plots of protein structures. J. Appl. Cryst. *24*, 946–950.

Merrit, E.A., and Murphy, M.E. (1994). Raster3D Version 2.0: a program for photorealistic molecular graphics. Acta Cryst. *D50*, 869–873.

Miller, P., DiOrio, C., Moyer, M., Schnur, R.C., Bruskin, A., Cullen, W., and Moyer, J.D. (1994). Depletion of the erbB-2 gene product p185 by benzoquinoid ansamycins. Cancer Res. *54*, 2724–2730.

Miller, S.J. (1995). I. The asymmetric synthesis of the antitumor antibiotic macbecin. Diss. Abstr. Int. [B] *55*, 3313.

Murakami, Y., Mizuno, S., and Uehara, Y. (1994). Accelerated degradation of 160 kDa epidermal growth factor (EGF) receptor precursor by the tyrosine kinase inhibitor herbimycin A in the endoplasmic reticulum of A431 human epidermoid carcinoma cells. Biochem. J. *301*, 63–68.

Nair, S.C., Toran, E.J., Rimerman, R.A., Hjermstad, S., Smithgall, T.E., and Smith, D.F. (1996). A pathway of multi-chaperone interactions common to diverse regulatory proteins: estrogen receptor, Fes tyrosine kinase, heat shock transcription factor Hsf1, and the aryl hydrocarbon receptor. Cell Stress and Chaperones *1*, 237–250.

Nathan, D.F., and Lindquist, S. (1995). Mutational analysis of Hsp90 function: interactions with a steroid receptor and a protein kinase. Mol. Cell. Biol. *15*, 3917–3925.

Nicholls, A., Sharp, K.A., and Honig, B. (1991). Protein Folding and association: insights from the interfacial and thermodynamic properties of hydrocarbons. Proteins Struct. Funct. Genet.*11*, 281–296.

Nieland, T.J.F., Tan, M.C.A.A., Monne-van Muijen, M., Koning, F., Kruisbeek, A.M., and Vanbleek, G.M. (1996). Isolation of an immunodominant viral peptide that is endogenously bound to the stress protein GP96/GRP94. Proc. Natl. Acad. Sci. USA *93*, 6135–6139.

Omura, S., Iwai, Y., Takahashi, Y., Sadakane, N., Nakagawa, A., Oiwa, H., Hasegawa, Y., and Ikai, T. (1979). Herbimycin, a new antibiotic produced by a strain of Streptomyces. J. Antibiot. (Tokyo) *32*, 255–261.

Ono, Y., Kozai, Y., and Ootsu, K. (1982). Antitumor and cytocidal activities of a newly isolated benzenoid ansamycin, macbecin I. Gann. *73*, 938–944.

Osborne, C.K., Yochmowitz, M.G., Knight, W.A., and McGuire, W.L. (1980). The value of estrogen and progesterone receptors in the treatment of breast cancer. Cancer *46*, 2884–2888.

Picard, D., Khursheed, B., Garabedian, B., Fortin, M.G., Lindquist, S., and Yamamoto, K.R. (1990). Reduced levels of hsp90 compromise steroid receptor action *in vivo*. Nature *348*, 166–168.

Pratt, W.B., and Welsh, M.J. (1994). Chaperone functions of the heat shock proteins associated with steroid receptors. Semin. Cell Biol. *5*, 83–93.

Rinehart, K.L., Jr., and Shield, L.S. (1976). Chemistry of the ansamycin antibiotics. Fortschr. Chem. Org. Naturst. *33*, 231–307.

Sasaki, K., Yasuda, H., and Onodera, K. (1979). Growth inhibition of virus transformed cells in vitro and antitumor activity in vivo of geldanamycin and its derivatives. J. Antibiot. (Tokyo) *32*, 849–851.

Schneider, C., Sepp-Lorenzino, L., Nimmesgern, E., Ouerfelli, O., Danishefsky, S., Rosen, N., and Hartl, F.U. (1996). Pharmacologic shifting of a balance between protein refolding and degradation mediated by Hsp90. Proc. Natl. Acad. Sci. USA *93*, 14536–14541.

Schnur, R.C., Corman, R.J., Gallaschum, R.J., Cooper, B.A., Dee, J.L., Doty, J.L., Muzzi, M.L., DiOrio, C.I., Barbacci, E.G., et al. (1995a). erbB-2 oncogene inhibition by geldanamycin derivatives: synthesis, mechanism of action, and structure-activity relationships. J. Med. Chem. *38*, 3813–3820.

Schnur, R.C., Corman, R.J., Gallaschum, R.J., Cooper, B.A., Dee, J.L., Doty, J.L., Muzzi, M.L., Moyer, J.D., DiOrio, C.I., Barbacci, E.G., et al. (1995b). Inhibition of the oncogene product p185(erbB-2) in vitro and in vivo by geldanamycin and dihydrogeldanamycin derivatives. J. Med. Chem. *38*, 3806–3812.

Schulte, T.W., Blagosklonny, M.V., Ingui, C., and Neckers, L. (1995). Disruption of the Raf-1–Hsp90 molecular complex results in destabilization of Raf-1 and loss of Raf-1–Ras association. J. Biol. Chem. *270*, 24585–24588.

Schumacher, R.J., Hurst, R., Sullivan, W.P., McMahon, N.J., Toft, D.O., and Matts, R.L. (1994). ATP-dependent chaperoning activity of reticulocyte lysate. J. Biol. Chem. *269*, 9493–9499.

Smith, D.F. (1993). Dynamics of heat shock protein 90–progesterone receptor binding and the disactivation loop model for steroid receptor complexes. Mol. Endocrinol. *7*, 1418–1429.

Smith, D.F., Whitesell, L., Nair, S.C., Chen, S.Y., Prapapanich, V., and Rimerman, R.A. (1995). Progesterone receptor structure and function altered by geldanamycin, an hsp90-binding agent. Mol. Cell Biol. *15*, 6804–6812.

Stancato, L.F., Chow, Y.H., Hutchison, K.A., Perdew, G.H., Jove, R., and Pratt, W.B. (1993). Raf exists in a native heterocomplex with hsp90 and p50 that can be reconstituted in a cell-free system. J. Biol. Chem. *268*, 21711–21716.

Stepanova, L., Leng, X., Parker, S.B., and Harper, J.W. (1996). Mammalian p50Cdc37 is a protein kinase–targeting subunit of Hsp90 that binds and stabilizes Cdk4. Genes Dev. *10*, 1491–1502.

Sullivan, W.P., and Toft, D.O. (1993). Mutational analysis of hsp90 binding to the progesterone receptor. J. Biol. Chem. *268*, 20373–20379.

Supko, J.G., Hickman, R.L., Grever, M.R., and Malspeis, L. (1995). Preclinical pharmacologic evaluation of geldanamycin as an antitumor agent. Cancer Chemother. Pharmacol. *36*, 305–315.

Tronick, S.R., and Aaronson, S.A. (1995). Growth factors and signal transduction. In The Molecular Basis of Cancer, J. Mendelsohn, P. Howley, M. Israel and L. Liotta, eds., pp. 117–140.

Wearsch, P.A., and Nicchitta, C.V. (1996). Endoplasmic reticulum chaperone GRP94 subunit assembly is regulated through a defined oligomerization domain. Biochemistry *35*, 16760–16769.

Whitelaw, M.L., Hutchison, K., and Perdew, G.H. (1991). A 50-kDa cytosolic protein complexed with the 90-kDa heat shock protein (hsp90) is the same protein complexed with pp60v-src hsp90 in cells transformed by the Rous sarcoma virus. J. Biol. Chem. *266*, 16436–16440.

Whitesell, L., and Cook, P. (1996). Stable and specific binding of heat shock protein 90 by geldanamycin disrupts glucocorticoid receptor function in intact cells. Mol. Endocrinol. *10*, 705–712.

Whitesell, L., Mimnaugh, E.G., De Costa, B., Myers, C.E., and Neckers, L.M. (1994). Inhibition of heat shock protein HSP90–pp60v-src heteroprotein complex formation by benzoquinone ansamycins: essential role for stress proteins in oncogenic transformation. Proc. Natl. Acad. Sci. USA *91*, 8324–8328.

Xu, Y., and Lindquist, S. (1993). Heat-shock protein hsp90 governs the activity of pp60v-src kinase. Proc. Natl. Acad. Sci. USA *90*, 7074–7078.

Zhu, X., Zhao, X., Burkholder, W.F., Gragerov, A., Ogata, C.M., Gottesman, M.E., and Hendrickson, W.A. (1996). Structural analysis of substrate binding by the molecular chaperone DnaK. Science *272*, 1606–1614.